

# The Influence of the AgNPs Ligand on the Antiviral Activity Against HSV-2

Emilia Tomaszewska<sup>1</sup>, Katarzyna Bednarczyk<sup>1</sup>, Martyna Janicka<sup>2,3</sup>, Marcin Chodkowski<sup>2</sup>,  
Małgorzata Krzyżowska<sup>2</sup>, Grzegorz Celichowski<sup>1</sup>, Jarosław Grobelny<sup>1</sup>, Katarzyna Ranożek-Soliwoda<sup>1</sup>

<sup>1</sup>University of Lodz, Faculty of Chemistry, Department of Materials Technology and Chemistry, Lodz, 90-236, Poland; <sup>2</sup>Military Institute of Hygiene and Epidemiology, Laboratory of Nanobiology and Biomaterials, Warsaw, 01-063, Poland; <sup>3</sup>Division of Microbiology, Department of Preclinical Sciences, Institute of Veterinary Medicine, Warsaw University of Life Sciences, Warsaw, 02-786, Poland

Correspondence: Katarzyna Ranożek-Soliwoda, University of Lodz, Faculty of Chemistry, Department of Materials Technology and Chemistry, Pomorska, 163, Lodz, 90-236, Poland, Tel +48 42 6354663, Fax +48 42 6355832, Email katarzyna.soliwoda@chemia.uni.lodz.pl

**Introduction:** In this paper, we discuss the influence of the ligand type present on the surface of silver nanoparticles (AgNPs) on its affinity to the virus surface and its virucidal activity against herpes simplex virus type 2 (HSV-2). We selected four different ligands, which potentially exhibit different affinity to the HSV-2 virus surface and used them for functionalization of AgNPs: i) sodium citrate; ii) tannic acid; iii) 1-mercaptopundecane-1-sulfonate (MUS); iv) and poly(ethylene glycol) (PEG).

**Methods:** The antiviral activity was performed by in vitro Vero cell culture. Anti-inflammatory activity was performed by measurement of NF-κB activity. The antiviral potential of functional NPs in vivo was tested with HSV-2 model of genital infection. Cryo- transmission electron microscopy (cryo-TEM) was used to directly visualize the interactions or lack of interactions of functional NPs with the surface of the HSV-2 virus and to assess their affinity for the virus surface.

**Results:** It was found that the surface chemistry of NPs plays a key role in modulation of its interaction with the HSV-2 virus. Two of the selected ligands (sodium citrate and PEG) were inert and show no affinity to the virus surface. AgNPs functionalized with heparan sulfate-mimic ligand (MUS) showed high affinity to the virus surface, and the appearance of these interactions resulted in virus deactivation in about 50%. In the case of silver nanoparticles functionalized with tannic acid, the assessment of the affinity is difficult to be resolved, mainly because TA-AgNPs exhibit very strong virucidal effect (~100%) and immediately after the contact of the HSV-2 virus with those NPs the virus structure is being destroyed.

**Discussion:** The obtained results indicate that the high affinity of functional nanoparticles to the virus surface does not provide the high virucidal effectiveness. The most effective revealed to be TA-AgNPs which exhibit very strong virucidal effect against HSV-2 virus.

**Keywords:** antiviral functional nanoparticles, interactions of nanoparticles with HSV-2, cryo-TEM, surface chemistry of antiviral nanoparticles

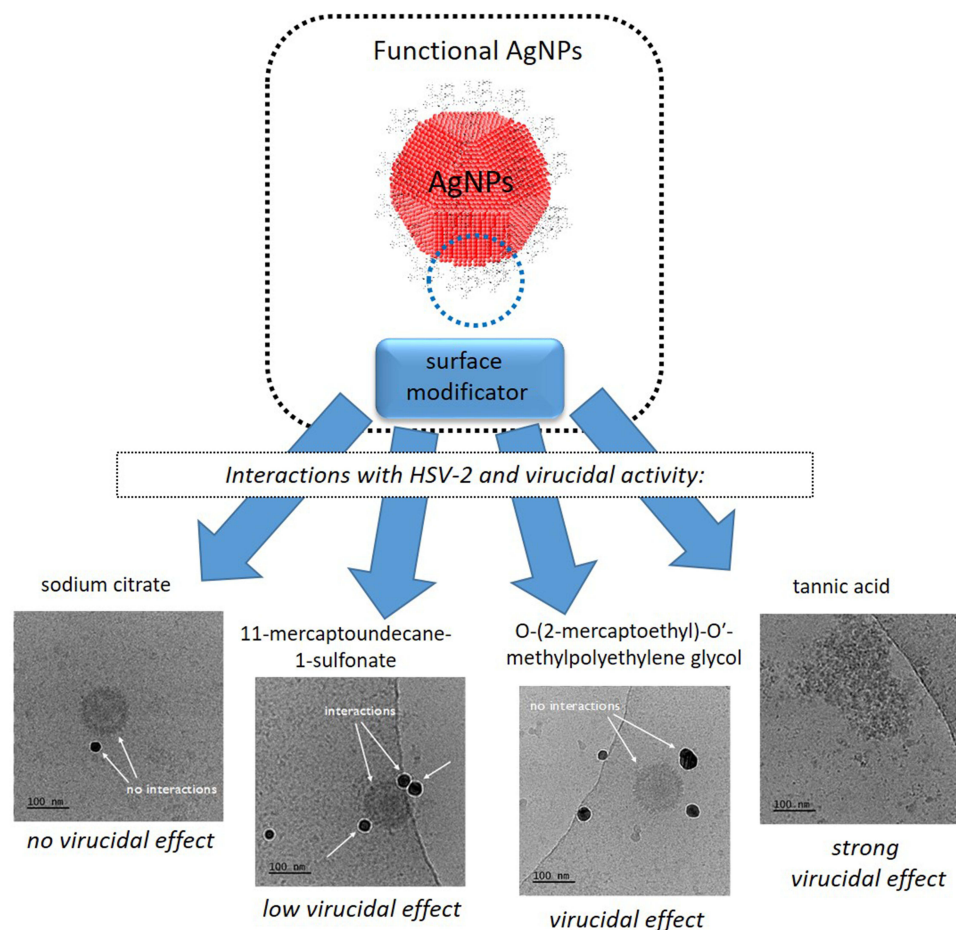
## Introduction

Human herpesviruses (HHV) are relatively common viruses. There are more than 100 known herpesviruses of which only 8 routinely infect humans: herpes simplex virus types 1 and 2, varicella-zoster virus, cytomegalovirus, Epstein-Barr virus, human herpesvirus 6 (variants A and B), human herpesvirus 7 and 8.<sup>1</sup> Of these, the HSV-1 and HSV-2 are the viruses that cause the herpes simplex (HSV) infection. The mucocutaneous manifestations of HSV infection include: gingivostomatitis, herpes genitalis, herpetic keratitis, and dermal whitlows.<sup>1</sup> The World Health Organization estimated

3.7 billion people under age of 50 (64%) globally have herpes simplex virus type 1 (HSV-1) infection, and 520 million people aged 15–49 (13%) worldwide have herpes simplex virus type 2 (HSV-2) infection.<sup>2</sup>

The HSV infection is transmitted only among people by direct contact. Also the perinatal infection is possible - from a pregnant woman to the newborn.<sup>3</sup> The virus replicates initially in epithelial cells, causing a characteristic vesicle on an erythematous base. It then ascends sensory nerves to the dorsal root ganglia, where, after an initial period of replication, it

## Graphical Abstract



establishes latency. It is not possible to completely cure HSV infection, because the common feature of herpesviruses is the development of a latent infection, ie a lifelong infection of the infected person, which means that one will always have herpesvirus in the body and periodically excrete it in saliva or genital secretions.<sup>1</sup> This is because, after entering the body, the virus multiplies and then travels along the nerves to sensory neurons (HSV-1 is most often located in the trigeminal ganglion, HSV-2 in the spinal ganglia), where it remains in a latent form ready to be reactivated under favourable conditions (exposure to strong sunlight, upper respiratory tract infections, fever fatigue, malnutrition, dental procedures, surgical operations or even stress). During reactivated infection, the virus spreads distally from the ganglion to initiate new cutaneous and/or mucosal lesions. The HSV reactivation may be asymptomatic, or it may increase the susceptibility to life-threatening disease.<sup>1</sup> The relationships between the herpes virus infections and events associated with neurodegeneration has been extensively studied.<sup>4-7</sup> Scientific evidence suggests that HSV-1 infection is involved in the pathogenesis of Alzheimer's disease (AD).<sup>7,8</sup> Kristen et al revealed that HSV-2 infection strongly alters the tau phosphorylation state and autophagic process in human neuroblastoma cells, leading to the appearance of AD-like neurodegeneration markers.<sup>7</sup>

The typical treatments for combating/mitigating HSV infection includes the antiviral drugs (acyclovir, denotivir, docosanol, tromantadine) in the case of mild lesions. In more severe forms of HSV infection the same antiviral drugs that inhibit the replication of virus are administered systemically (orally or intravenously). However, those drugs reduce only the symptoms of primary and recurrent infection, but do not eliminate latent virus and do not reduce the risk of infecting others or the frequency and severity of relapses after discontinuation of treatment.

Nanomaterials, including nanoparticles (NPs), are of great interest in combating viral infection.<sup>9</sup> What's more, research shows that the action of NPs can be multifaceted. NPs, apart from strong virucidal properties, can also act as adjuvants, reducing the frequency of recurrences of viral infection,<sup>10–12</sup> and modulating biofilm formation.<sup>13</sup> Moreover, the interactions of functional NPs with viruses can be multimodal due to their small size and possibility of functionalization. The effectiveness of functional NPs as antiviral agents depends on many factor including: the type of nanoparticle (gold, silver,<sup>14–16</sup> emulsomal NPs,<sup>17,18</sup> nano-biosomes<sup>19</sup> etc.), the size of the NPs,<sup>20,21</sup> but also, and perhaps mainly, on the type of ligands present on the surface of the NPs, which are the real participant of the NPs interactions with viruses.<sup>20</sup> The ligands/modifiers present on the surface of NPs provide them colloidal stability and prevent against agglomeration and/or aggregation processes, but also properly selected ligands, can be used to tune the interactions of NPs with the surrounding environment.

The structure of herpesviruses consist of a core containing a double-stranded DNA genome which is enclosed by an icosapentahedral capsid composed of capsomers.<sup>1</sup> The capsid is surrounded by an amorphous protein coating called the tegument which is encased in a glycoprotein-bearing lipid bilayer envelope. These glycoproteins confer distinctive properties to each virus and provide unique antigens to which the host is capable of responding. Through the appropriate NPs ligands, those virus-host cell interactions can be disturbed and hence, the processes of docking and fusion of the virus to the host cell can also be disrupted. There are several scientific reports that indicate the crucial role of the ligands present on the surface of NPs in the construction of virucidal agents based on nanomaterials.<sup>20–22</sup> Papp et al<sup>22</sup> showed that the binding of the viral fusion protein hemagglutinin to the host cell surface is mediated by sialic acid receptor and the use of sialic-acid-functionalized AuNPs competitively inhibit viral infection. Cagno et al<sup>23</sup> showed that proper functionalization of NPs with linkers mimicking heparan sulfate proteoglycans can target the viral attachment ligands. Such ligands adsorbed on the surface of NPs increase the affinity of NPs to the surface of the HSV. Such competitive action of functional NPs reduces the possibility of infection of the host cell. The antiviral action of functional NPs can also be carried out by blocking the viral proteins responsible for docking and fusing the virus into the host cell.<sup>21</sup> However, this approach based on the lowering of the virus binding on cells by blocking the virus receptors with functional NPs leads to 40% reduction of infection.<sup>21</sup> Such functional NPs exhibit affinity to the virus surface, blocking the docking to the appropriate receptors, but they had essentially no virucidal effect. Studies also indicate that modifications can also increase the virucidal activity of polyphenols, eg curcumin<sup>17</sup> or bioavailability of active compounds.<sup>24</sup>

In our previous work,<sup>22</sup> we have shown that tannic acid-modified AgNPs (13 nm, 33 nm and 46 nm) are effective in reducing HSV-2 infectivity both in vitro and in vivo, and the effectiveness of blocking virus attachment depends on the size of those nanoparticles. Moreover, we revealed that this antiviral effect is more efficient for tannic acid-modified nanoparticles than the tannic acid itself.<sup>22</sup> This effect was observed in terms of blocking virus attachment, penetration and cell-to-cell spread after initial infection. However, in this work, we did not investigate the effect of different ligands but only different sizes of nanoparticles functionalized with same nanoparticles surface chemistry. Although, scientific results confirm the importance of surface ligands in nanoparticle-virus interactions<sup>20–22</sup> there is a lack of systematic information about the comparison of the most commonly used ligands and its influence on the affinity of modified-NPs on its antiviral activity against HSV-2.

In this paper, we discuss the influence of the type of ligand present on the surface of silver nanoparticles (AgNPs) with the size of about 30 nm on its virucidal activity against herpes simplex virus type –2 (HSV-2). We selected four different ligands for AgNPs: i) sodium citrate (SC); ii) tannic acid (TA); iii) 1-mercaptopundecane-1-sulfonate (MUS); iv) and (O-(2-mercaptopethyl)-O'-methylpolyethylene glycol (PEG) (see Graphical Abstract). Functional NPs were precisely characterized with dynamic light scattering (DLS) and high-resolution scanning transmission electron microscopy (HR-STEM). The antiviral activity of functional NPs against HSV-2 virus was studied by using VERO cell line. Anti-inflammatory activity was analyzed through the measurement of NF- $\kappa$ B activity. The antiviral potential of functional NPs in vivo was tested with HSV-2 model of genital infection. Cryo- transmission electron microscopy (cryo-TEM) was used to directly visualize the interactions of functional NPs with the HSV-2 virus and to assess their affinity for the virus surface and its virucidal effect.

## Materials and Methods

### Chemicals

Silver nitrate ( $\text{AgNO}_3$ , purity 99.999%, Sigma-Aldrich, St. Louis, MO, USA), sodium citrate ( $\text{C}_6\text{H}_5\text{Na}_3\text{O}_7 \cdot 2\text{H}_2\text{O}$ , purity 99.0% Sigma-Aldrich), tannic acid ( $\text{C}_{76}\text{H}_{52}\text{O}_{46}$ , Sigma Aldrich), sodium 11-mercaptoundecane-1-sulfonate (MUS,  $\text{C}_{11}\text{H}_{23}\text{NaO}_3\text{S}_2$ , Prochimia, Poland), O-(2-mercaptoethyl)-O'-methylpolyethylene glycol (PEG-SH, Mw=6000, Sigma Aldrich), sodium borohydride ( $\text{NaBH}_4$ , purity  $\geq 96\%$ , Sigma-Aldrich) were used as received. For all preparations, deionized water obtained from the Deionizer Millipore Simplicity UV system (specific resistivity of water was  $18.2 \text{ M}\Omega\cdot\text{cm}$ ) was used.

### Nanoparticles Synthesis

#### Citrate-Modified AgNPs (SC- AgNPs)

Citrate modified-AgNPs with the mean size of metallic core equal to 30 nm were prepared according to seed growth-mediated method, which is a two-step procedure.<sup>20</sup> Firstly, silver seeds were synthesized, and were then used to prepare the final AgNPs with the size equal to 30 nm. The synthesis procedure was as follows: sodium citrate (0.228 g) and deionized water (95 g) were mixed in the flask and heated at  $70^\circ\text{C}$  for 15 min. Next, silver nitrate (1.7 mL, 1%) was added, and then sodium borohydride (2 mL, 0.1%) was added with the syringe pump (syringe capacity 2 mL, diameter 8.00 mm, flow rate  $55 \text{ mL}\cdot\text{h}^{-1}$ ). Next, the whole mixture was additionally heated for 60 min at  $70^\circ\text{C}$ , and then cooled down to room temperature. The synthesis procedure was carried out without reflux thus after the synthesis process, the amount of deionized water was added by weight so that the colloid mass was finally equal 100 g and the metal concentration equal 100 ppm. In the second step of the synthesis process: sodium citrate (3 g, 1%) and deionized water (75 mL) were heated for 15 min under reflux. Next, into the mixture solution silver seeds were added (10 g) and an aqueous solution of silver nitrate with the syringe pump (2.6 mL, syringe 10 mL, diameter 10 mm, flow 20 mL/h). The whole mixture was heated for 1 hour under reflux and next the second portion of sodium citrate was added (3 mL, 1%) and the second portion of silver nitrate with a syringe pump (2.6 mL, syringe 10 mL, diameter 10 mm, flow 20 mL/h), and the mixture was heated for another 60 min. In the last step, the colloid was cooled down to the room temperature. The final AgNPs concentration was 355 ppm, and for all experiments this colloid was diluted to 100 ppm.

#### Tannic Acid -Modified AgNPs (TA-AgNPs)

Tannic acid -modified AgNPs were synthesized according to chemical reduction method already described in our previous work.<sup>20</sup> Briefly, to the silver nitrate solution (95.2 g, 0.017%) warmed to the boiling point a mixture of aqueous solution of sodium citrate (4.2 g, 4%) and tannic acid (0.6 g, 5%) was added. Immediately after the reagent's incorporation, the solution's color changed to brown, indicating the formation of silver nanoparticles. The solution was vigorously stirred under reflux for an additional 15 min and cooled down to room temperature. The concentration of nanoparticles in colloid was equal to 100 ppm.

#### O-(2-Mercaptoethyl)-O'-Methylpolyethylene Glycol -Modified AgNPs (PEG-AgNPs)

PEG-AgNPs with the mean size of metallic core equal about 30 nm were prepared by the use of TA-AgNPs colloids. The modification was performed according to modified procedure already described in.<sup>25</sup> Briefly, this colloid was centrifuged to remove TA a next the NPs were functionalized of with O-(2-mercaptoethyl)-O'-methylpolyethylene glycol (PEG). Briefly, into the 1 g of colloid an aqueous solution of PEG (0.03354 g; 0.17%) and the colloid was left for 24 h for surface functionalization. The amount of PEG molecules per  $1 \text{ nm}^2$  of NPs surface was equal 3.

#### 11-Mercaptoundecane-1-Sulfonate -Modified AgNPs (MUS-AgNPs)

MUS-modified AgNPs were prepared according to procedure already presented in our previous work in.<sup>20</sup> Briefly, to the 5 g of citrate-AgNPs colloid with the metal concentration equal 100 ppm and the size of metallic core of about 30 nm and 0.04599g of 0.05% aqueous solution of MUS was added and the colloid was left for 24 h for ligand exchange. The surface coverage of AgNPs with MUS was equal 5 molecules per  $1 \text{ nm}^2$  of NP.

## Methods

### Nanoparticles Characterization

The characterization of functional nanoparticles SC-AgNPs, PEG-AgNPs, MUS-AgNPs and TA-AgNPs was performed using: Dynamic Light Scattering (DLS, Litesizer 500, Particle Analyzer, Anton Paar), High-Resolution Scanning Electron Microscopy equipped with transmission detector STEM II (HR-STEM, NovaNanoSEM 450, FEI, USA). STEM samples were prepared by drop-casting an aqueous dispersion of the NPs colloid onto carbon-coated copper grids. The size distribution of the NPs was analyzed by measurement of at least 500 nanoparticles for each sample, and the histogram for the size distribution of particles was prepared.

### Virus and Antiviral Tests

Laboratory strains of HSV-1 (strain McKrae) and HSV-2 (strain 333)<sup>12</sup> were grown and titrated in Vero cells (ATCC® CCL-81, Rockville, MD, USA). All anti-viral tests were also performed in Vero cells. Virus was diluted in MEM (Thermo Fisher Scientific, Waltham, MA, USA) and kept on ice before use. Vero cells were cultured in DMEM complete medium (10% fetal calf serum, 10 U/mL penicillin, and 100 µg/mL streptomycin, Thermo Fisher Scientific) in 24-well plates until reaching 95% confluence. Antiviral activity of AgNPs was studied by incubating HSV-1 or -2 with a fixed dose (100 PFU/mL) for 60 min with 7.5 µg/mL or 2.5 µg/mL of AgNPs in culture medium. Next, the mixture was added to Vero cells for 60 min at 37 °C, after which cultures were washed with cold PBS, and 2% methylcellulose in complete culture medium was added. Twenty-four hours later, plates were washed, stained with 1% crystal violet and counted for the number of plaques. Data were expressed as % of infection (in %) using the equation;  $100 \times [(\text{number of plaques with treatment})/(\text{number of plaques without treatment})]$ .

### Activation of NF-κB

RAW-Dual™ (IRF-Lucia/KI-[MIP-2]SEAP) cells (InvivoGen, Toulouse, France) were used to measure NF-κB activity. Cells were grown in DMEM complete medium (10% fetal calf serum, 10 U/mL penicillin, and 100 µg/mL streptomycin, Thermo Fisher Scientific) in 96-well plate overnight. The next day, cells were stimulated with poly I:C (0,1 µg/mL) and AgNPs at 5 µg/mL for 6 h. The activity of SEAP (secreted embryonic alkaline phosphatase) was measured in the supernatant using QUANTI-Blue™ Solution (InvivoGen).

### In vivo Experiments

To check anti-viral potential in vivo, HSV-2 model of genital infection was used, as described before.<sup>11</sup> Shortly, female, 6- to 8-week-old C57BL/6 mice were used for all experiments. For genital HSV-2 Infection, female mice were injected s. c. (subcutaneous) with 2.0 mg/mouse of medroxyprogesterone (Depo-Provera; Pfizer, Puurs, Belgium) in 200 µL of PBS. Five days later, the mice were anesthetized and inoculated intravaginally with 20 µL of PBS containing 10<sup>3</sup> PFU of HSV-2 strain 333. Vaginal washings were performed at 24, 48 and 72 h after infection with 200 µL of 0.9% NaCl solution containing 10 µg/mL AgNPs or 0.9% NaCl solution. The vaginal washings obtained at 72 h after infection were subjected to HSV-2 titration by qPCR, as described before.<sup>26</sup> The animal study protocol was approved by the Local Committee on the Ethics of Animal Experiments in Warsaw, Poland (permit Number: WAW2/69/2021). The study was performed in strict accordance with the recommendations of the Polish Act of 21 January 2005 on animal experiments (OJ no 33, item 289) and Directive 2010/63/EU of the European Parliament and the Council of 22 September 2010 on the protection of animals used for scientific purposes. Mice were monitored daily and those showing neurological symptoms or significant weight loss (>25%) were immediately removed from the experiment.

### Interactions of Functional Nanoparticles With HSV-2

Cryogenic Transmission Electron Microscopy (cryo-TEM) images were obtained using a Tecnai F20 X TWIN microscope (FEI Company, Hillsboro, Oregon, USA) equipped with field emission gun, operating at an acceleration voltage of 200 kV. Images were recorded on the Gatan Rio 16 CMOS 4k camera (Gatan Inc., Pleasanton, California, USA) and processed with Gatan Microscopy Suite (GMS) software (Gatan Inc., Pleasanton, California, USA). Specimen preparation was done by vitrification of the aqueous solutions on grids with holey carbon film (Quantifoil R 2/2; Quantifoil Micro Tools GmbH, Großlobichau, Germany). Prior to use, the grids were activated for 15 seconds in oxygen plasma using a Femto plasma cleaner (Diener Electronic, Ebhausen, Germany). Cryo-samples were prepared by applying



a droplet (3  $\mu$ L) of the suspension to the grid, blotting with filter paper and immediate freezing in liquid ethane using a fully automated blotting device Vitrobot Mark IV (Thermo Fisher Scientific, Waltham, Massachusetts, USA). After preparation, the vitrified specimens were kept under liquid nitrogen until they were inserted into a cryo-TEM-holder Gatan 626 (Gatan Inc., Pleasanton, USA) and analyzed in the TEM at  $-178^{\circ}\text{C}$ .

### Statistics

Data were analyzed using GraphPad Prism version 7 (GraphPad software). The statistical tests included: an unpaired Student's *t*-test (normal distribution) or the Mann–Whitney *U*-test and the results are reported as mean  $\pm$  standard error of the mean (SEM) unless indicated otherwise. The  $p \leq 0.05$  was considered statistically significant.

## Results and Discussion

The size and shape of functional AgNPs (SC-AgNPs, PEG-AgNPs, MUS-AgNPs and TA-AgNPs) were determined with HR-STEM (Figure 1). The hydrodynamic size and the colloidal stability of functional NPs was investigated with DLS technique.

The functional NPs have been designed so that the size of the metallic core was comparable in each case. The shape and size of the metal core were equal within the statistical error for all types of functional NPs. AgNPs had a spherical shape and the size of metallic core was equal to  $25 \pm 5$  nm (SC-AgNPs, Figure 1A),  $27 \pm 7$  nm (PEG-AgNPs, Figure 1B),  $25 \pm 6$  nm (MUS-AgNPs, Figure 1C) and  $27 \pm 7$  nm (TA-AgNPs, Figure 1D). The hydrodynamic size of functional nanoparticles measured with DLS varied depending on the ligand type present on the surface of the metallic AgNPs (Figure 1A–D). The smallest hydrodynamic diameter was measured for SC-AgNPs ( $d_H = 31 \pm 8$  nm, Figure 1A) that contains citrate ligand and MUS-AgNPs ( $d_H = 31 \pm 6$  nm, Figure 1C) with 11-mercaptoundecane-1-sulfonate. In the case of larger ligand such as TA and PEG the hydrodynamic diameter was equal to  $d_H = 38 \pm 7$  nm (TA-AgNPs, Figure 1D)

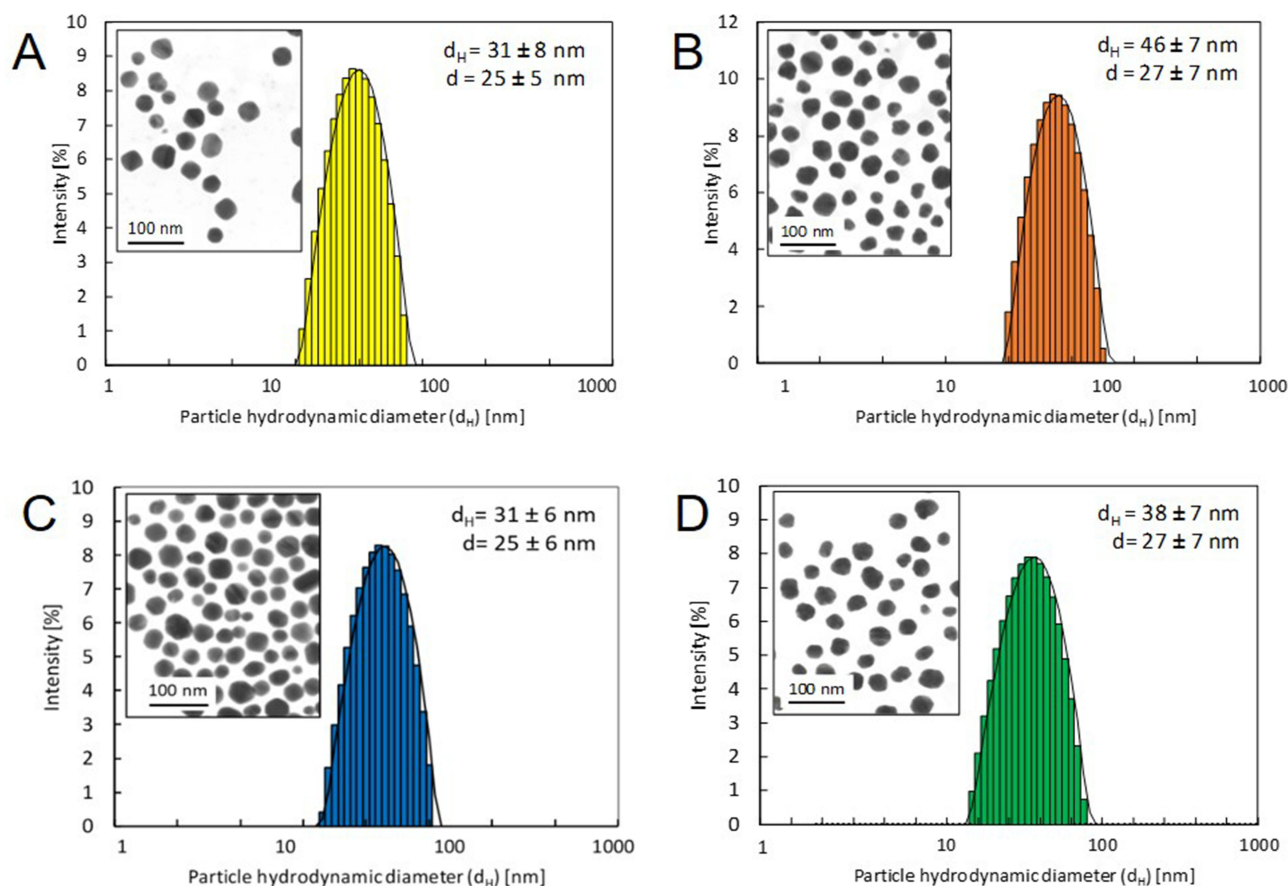


**Figure 1** The DLS size distribution histograms and HR-STEM images of functional nanoparticles: SC-AgNPs-SC (A); PEG-AgNPs (B); MUS-AgNPs (C) TA-AgNPs-TA (D).

**Table 1** The Overall Results of AgNPs Characterization Results (d<sub>H</sub>- Hydrodynamic Diameter From DLS Measurements, d- the Size of Nanoparticle Metallic Core Measured With HR-STEM)

Functional NPs	d <sub>H</sub> [nm] (DLS)	d <sub>STEM</sub> [nm] (HR-STEM)
SC-AgNPs	31 ± 8 nm	25 ± 5 nm
PEG-AgNPs	46 ± 7 nm	27 ± 7 nm
MUS-AgNPs	31 ± 6 nm	25 ± 6 nm
TA-AgNPs	38 ± 7 nm	27 ± 7 nm

and d<sub>H</sub> = 46 ± 7 nm (PEG-AgNPs, Figure 1B). All colloids were stable and any aggregates or agglomerates were not detected. The overall results of functional nanoparticles characterization are shown in Table 1.

Cytotoxicity of functional AgNPs was first characterized with MTT test (Table 1S, Supplementary Material). We selected two concentrations of functional AgNPs (2.5 and 7.5 µg/mL) on the basis of our previous works,<sup>20,22,24</sup> but also to check the lowest concentration showing no cytotoxic activity for cells able to internalize AgNPs. The antiviral properties of functional AgNPs were first tested by the standard plaque forming assay (PFU/mL) in Vero cell culture. Incubation of HSV-2 with functional AgNPs prior to cells infection showed significant inhibition of HSV-2 infection by all tested functional AgNPs ( $p \leq 0.05$ ) (Figure 2), while SC-AgNPs showed no antiviral activity. We observed that MUS-AgNPs were less effective against HSV-2 compared to TA-AgNPs and PEG-AgNPs (Figure 2). The IC<sub>50</sub> values for TA-AgNPs, PEG-AgNPs and MUS-AgNPs were 1.18 ± 0.16, 1.87 ± 0.2, and 6.55 ± 1.1, respectively.

NF-κB represents a family of inducible transcription factors, the activation which leads to coordinated expression of many genes that encode cytokines, chemokines and adhesion molecules involved in regulation of immune response and inflammation.<sup>27</sup> Excessive inflammation during HSV-1/2 leads to deregulation of the local antiviral immune response both at the level of mucosal tissue and nervous tissues.<sup>28,29</sup> AgNPs sized >20 nm have been shown to down-regulate eternally induced inflammatory response in cancer cells.<sup>30</sup> Therefore, we measured NF-κB activity using in vitro assay after 18 h exposition to each functional AgNPs in cells previously treated with poly (I:C) or infected for 6 h with HSV-1 or HSV-2. The measurements of NF-κB activity showed that any modification of AgNPs leads to significant down-regulation of TLR3-dependent activation of NF-κB activity ( $p \leq 0.01$ ) (Figure 3). Poli (I:C) is a homolog of viral dsRNA

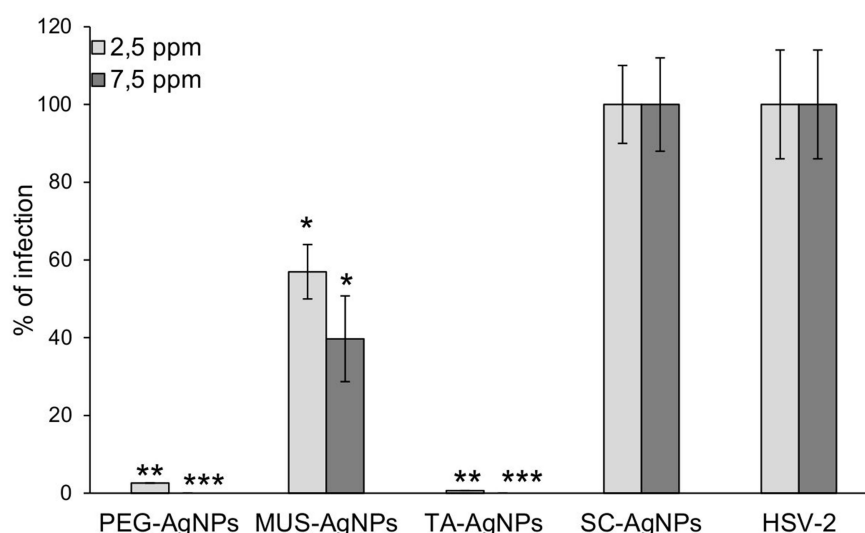


**Figure 2** Functional-AgNPs inhibit HSV-2 infection in vitro. HSV titers (PFU/mL) in Vero cells infected with HSV-2 pre-incubated for 1 h with SC-AgNPs, PEG-AgNPs, MUS-AgNPs and TA-AgNPs functional (7.5 µg/mL or 2.5 µg/mL of functional-AgNPs). The data are expressed as means from three independent experiments ± SEM. \*\*\*represents significant differences with  $p \leq 0.001$ , \*\*with  $p \leq 0.01$ , and \*with  $p \leq 0.05$  in comparison to infected control.

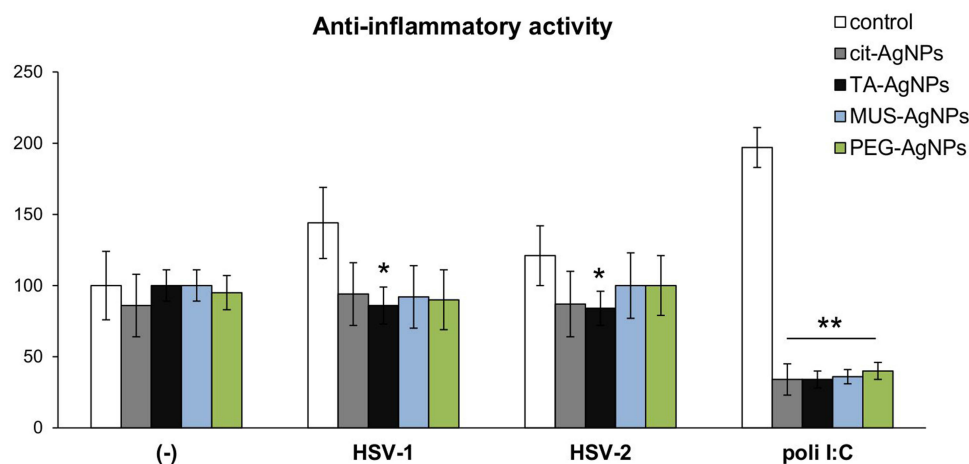


**Figure 3** Anti-inflammatory activity upon AgNPs treatment measured in RAW-Dual™ (IRF-Lucia/KI-[MIP-2] SEAP) cell. Two-way ANOVA test. \*Represents  $p \leq 0.05$ , and \*\* $p \leq 0.01$  in comparison to untreated control, either uninfected, HSV-1/2-infected or poly (I:C)-treated.

and activator of TLR3-dependent inflammatory and antiviral pathways (Figure 3). Interestingly, only TA modification was able to down regulate HSV-induced NF- $\kappa$ B activity, indicating that other specific pathways induced by HSV-1/2 infection are not sensitive to AgNPs ( $p \leq 0.05$ ) (Figure 3). Vendidandala et al<sup>31</sup> demonstrated that the use another polyphenolic compound, such as gallic acid (GA) to modify silver nanoparticles suppresses oxidative stress and inflammation via modulating the Nrf2/HO-1 and TLR4/NF- $\kappa$ B pathways.

The RAW cells were uninfected, infected with HSV-1 (100 PFU/cell) or treated with poly (I:C) at 0.1  $\mu$ g/mL for 6 h, then AgNPs were added at 5  $\mu$ g/mL for 6 h. After 6 h, activation of NF- $\kappa$ B pathway was measured as SEAP activity. Data from three independent experiments are presented as mean  $\pm$  SEM. Two-way ANOVA test. \* Represents  $p \leq 0.05$ , and \*\*  $p \leq 0.01$  in comparison to untreated control, either uninfected, HSV-1/2-infected or poly (I:C)-treated.

To study how local application of AgNPs can be used for treatment of HSV-2 infection, we applied intravaginally 200  $\mu$ L of 0.9% NaCl solution containing 10  $\mu$ g/mL AgNPs or 0.9% NaCl solution at 24, 48 and 72 h after infection. The vaginal washings at 72 h were subjected to HSV-2 titration by qPCR (Figure 4). Treatment of HSV-2 mucosal infection with functional AgNPs showed that only TA- and PEG-modified AgNPs were able to significantly reduce the HSV-2 titers in vaginal tissues ( $p \leq 0.05$ ) (Figure 4). However, activity of PEG-modified AgNPs was weaker in comparison to TA-AgNPs.

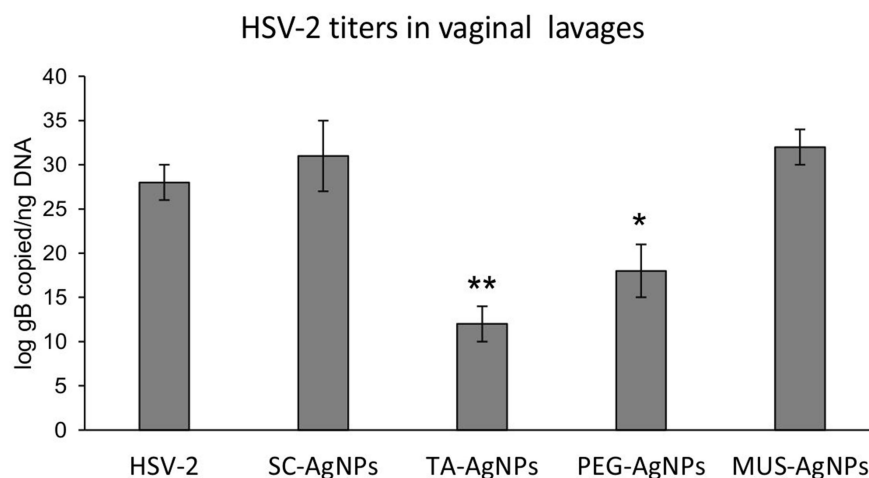


**Figure 4** HSV-2 titers in vaginal lavages collected after 3 treatments with SC-AgNPs, TA-AgNPs, PEG-AgNPs or MUS-AgNPs or NaCl (HSV-2) at 72h post infection. HSV-2 gB titers (copies/ng DNA) were measured by qPCR (N = 6). The bars represent means  $\pm$  SEM. \*represents significant differences with  $p \leq 0.05$ , \*\* $p \leq 0.01$  in comparison to untreated infected tissues.



The cryo-TEM studies were carried out to investigate the influence of surface chemistry and ligands type present on the surface of AgNPs on the affinity of the functional NPs to HSV-2 virus. For this purpose, the functional AgNPs were incubated with the HSV-2 virus for 30 seconds and next visualized using the cryo-TEM technique. Figure 5 presents the cryo-TEM images of HSV-2 virus without NPs. The cryo-TEM images revealed the hexagonal shape of icosapentahedral structure of the virus with clearly visible glycoprotein spikes (Figure 5A). The Schiffer and Corney<sup>32</sup> described the structure of the HSV-2 virus as enveloped virus with the size about 160 nm in diameter. In our measurements, the mean diameter of the HSV-2 virus is equal about 120 nm (Figure 5B).

The cryo-TEM images of HSV-2 virus after the incubation with functional NPs are presented in Figure 6.

The cryo-TEM images revealed that the SC-AgNPs do not attach to the surface of NPs which is related to the lack of affinity of the citrate ligand for HSV-2 virus proteins (Figure 6A). Moreover, these functional nanoparticles exhibit no virucidal effect (Figure 2) and no anti-inflammatory activity (Figure 3). SC-AgNPs were also unable to reduce the HSV-2 titers in tissues (Figure 3). This low biological activity of these functional NPs is related to the type of ligand present on the surface of the NPs. SC has no affinity for the spike proteins on the HSV-2 virus and does not have a virucidal effect on its own. SC-AgNPs do not show significant virucidal activity against HSV-2, which most probably is the consequence of the lack of its affinity to virus surface. The analysis of cryo-TEM images revealed that PEG-AgNPs are isolated and do not exhibit affinity for the virus protein surface. We observed the NPs separated from the virus and it is clear that there are no interactions between PEG-AgNPs and HSV-2 virus. The PEG is a non-ionic polyether compound, hence there is no possibility of ionic or electrostatic interactions between the polymer and the virus. However, in our study PEG-modified AgNPs showed very good antiviral activity in vitro (Figure 2). The fact that PEG-ylation might enhance the antiviral activity and reduce the cytotoxicity of NPs as it was also presented by Ghaffari et al<sup>33</sup> who presented higher antiviral potential of PEG-ylated ZnONPs than unmodified ZnONPs against H1N1 influenza virus. In the case of MUS-AgNPs the multiple attachment of the NPs to virus can be clearly visible (Figure 6C). The MUS-AgNPs are associated with the HSV-2 virus confirming the interaction of MUS-ligand with HSV-2 viral proteins. The interaction of MUS-AgNPs are based on the heparin-mimic compound (MUS-ligand) which ensures the electrostatic attraction with virus surface by the negative charge of sulfone group. It is already well-known that the cell surface carbohydrate moieties frequently serve as initial receptors for viruses.<sup>34</sup> Sulfated, sulfonated, and carboxyl-containing agents are able to inhibit a large number of viruses, especially the ones whose viral attachment ligands seeks heparan sulfate proteoglycans.<sup>35–37</sup> Moreover, ligands rich in sulfated sequences are considered to be the strongest binders to heparin binding proteins.<sup>38</sup> In HSV-2 virus at least two proteins: glycoprotein C (gC-2) and glycoprotein B (gB-2) were demonstrated to be able to bind heparin.<sup>39–41</sup> This affinity results in a large amount of MUS-AgNPs to be observed directly on the virus surface. Moreover, heparan sulfate mimic linkers may have a virucidal effect by targeting viral attachment ligands. MUS-modified AgNPs showed only about 50% of antiviral activity in vitro (Figure 2) which indicate rather virustatic that virucidal mechanism of action of MUS-AgNPs. This fact we already presented in our previous work.<sup>20</sup> Very strong

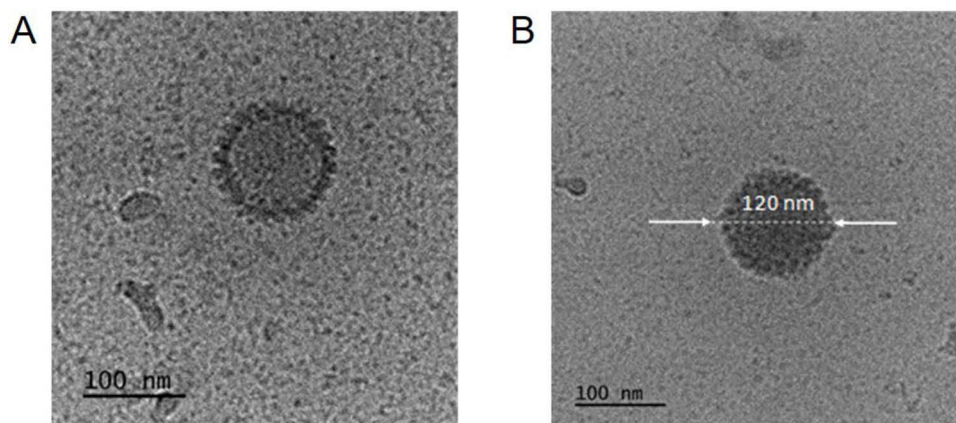


**Figure 5** Cryo-TEM images (**A** and **B**) of HSV-2 virus (unstained sample). The measured diameter of the HSV-2 virus is equal 120 nm (**B**).

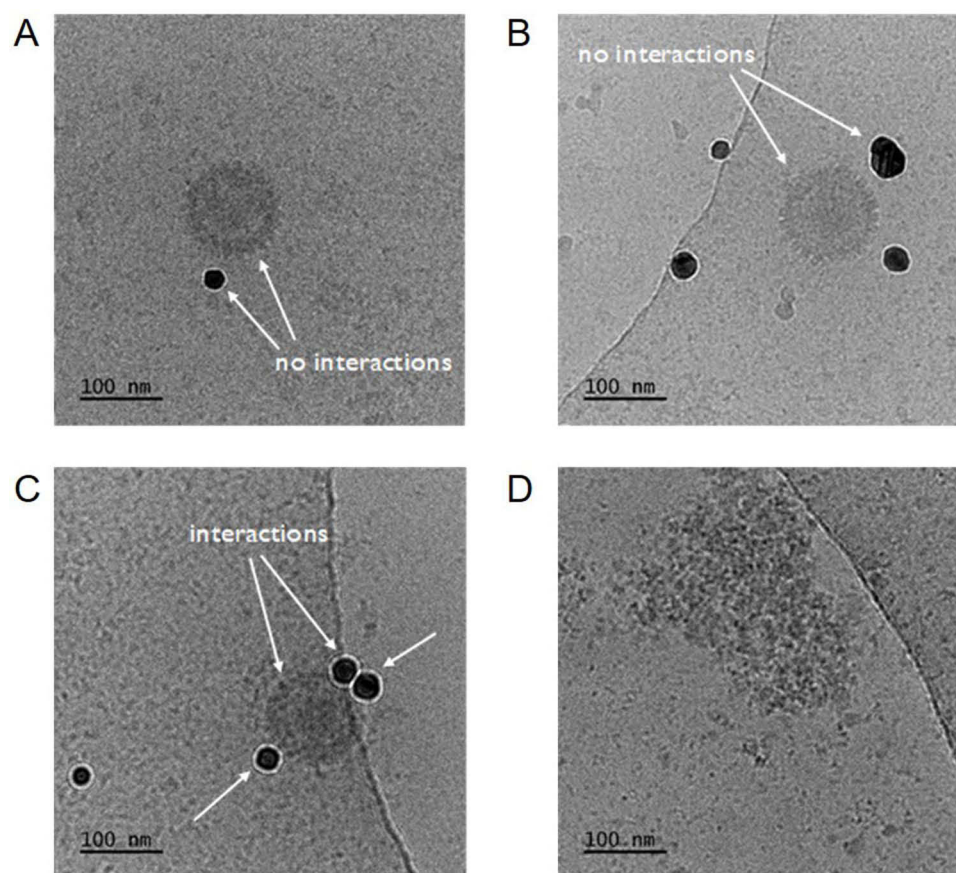


**Figure 6** Cryo-TEM images of unstained samples: HSV-2 virus after incubation with: SC-AgNPs (A), PEG-AgNPs (B) MUS-AgNPs (C) and TA-AgNPs (D). Samples imaged after about 30s of incubation of virus with functional nanoparticles. Images presenting the interaction of functional nanoparticles with HSV-2 surface.

virucidal effect is observed in case of the TA-AgNPs (Figures 6D, 7A and B). Most probably TA chemically damage the virus structure which result in very fast and the strongest virucidal effect (Figure 2). Treatment of HSV-2 mucosal infection with functional AgNPs showed that TA- modified AgNPs reduces the most HSV-2 titers in tissues along all investigated functional NPs (Figure 3). TA contains domains composed of closely packed repeating units - gallic acids. It is well-known that most viral attachment ligands (VALs) also possess closely packed repeating units, hence they are ideally suited for multivalent binding to their cell receptor. Moreover, TA may bind very tightly to proteins by forming

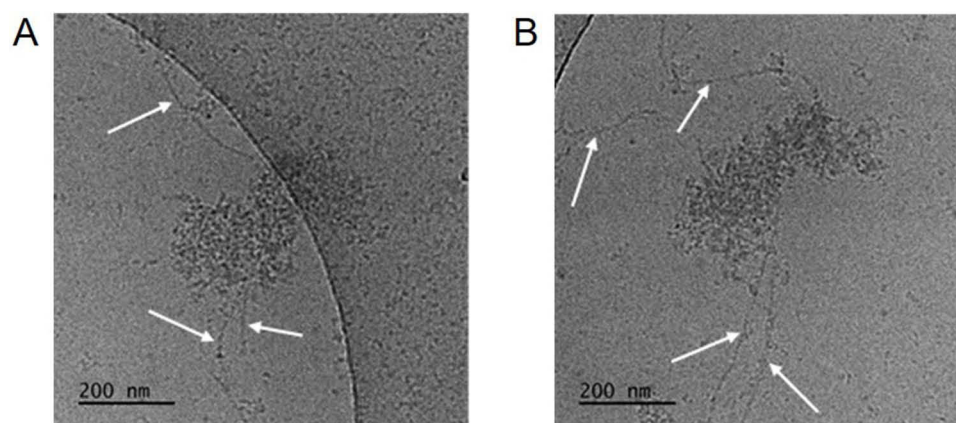


**Figure 7** Cryo-TEM images of damaged HSV-2 structure after exposition to TA-AgNPs (A and B) (30s of exposition, samples unstained; arrows indicate the separated strands of the DNA helix from destroyed structure of HSV-2 viruses).

multiple hydrogen bonds between their phenolic groups and the -NH groups of the peptides.<sup>42</sup> Hence, TA, due to its structure, can also interact with the proteins on the surface of the virus. Lin et al<sup>43</sup> also identified hydrolysable tannins as compounds that inhibit viral glycoprotein interactions with cell surface glycosaminoglycans (GAGs). The strong multi-valent binding of TA-AgNPs to HSV-2 virus membrane may lead to local distortions<sup>44,45</sup> and consequently cause the global virus deformation, and irreversible loss of virus infectivity. TA-AgNPs and HSV-2 interactions may result in damage of the envelope of viruses and therefore, leading to a damage of the capsid with the releasement of viral genetic material. The analysis of the cryo-TEM images of destroyed HSV-2 viruses revealed the presence of separated strands of the DNA helix (Figure 7A and B). These images clearly indicate that the veridical action of TA-AgNPs against HSV-2 viruses causes the destruction of the virus structure but also the unwinding of the DNA strands.

The main difference between MUS- and TA-ligand is that the TA-AgNPs exhibit virucidal effect and are able to affect the structural integrity of the virus, while MUS-AgNPs attach to the virus and exhibit much less virucidal activity. This finding was also observed by Isenburg et al<sup>42</sup> who revealed the antiviral effects of hydrolysable and galloylated condensed tannins due to inhibition of virus adsorption. Xie et al<sup>46</sup> suggested that the inhibition action of tannins could be due to its binding to components of the viral envelope, preventing viral attachment and penetration of the plasma membrane. The ellagitannin as casuarinin was also found to possess anti-herpesvirus activity in inhibiting viral attachment to cells and viral penetration, and also disturbing the late events of infection.<sup>46</sup> Also, studies by Fukuchi et al<sup>47</sup> on the mode of anti-HSV action hypothesized that TA inhibits virus attachment to cells. Reshamwala et al<sup>48</sup> showed that polyphenols exert their antiviral effect through binding to multiple sites on the virion surface, leading to aggregation of the virions and preventing RNA release and reducing cell surface binding. The two hydrolysable tannins (chebulagic acid and punicalagin) were found to exhibit inhibitory effect of HSV type 1 (HSV-1), especially in entry and spread stage of the virus.<sup>49</sup> The authors revealed that tannins can bind to viral glycoproteins on viruses and the cell surfaces of infected cells, blocking virus attachment, entry, and cell to cell spread. Authors also showed that tannins may target more than one step of infection, including attachment, membrane fusion, and cell-to-cell fusion. We may also conclude that the character of binding between tannins and HSV glycoproteins may help to induce better immune response by acting as nanoadjuvants facilitating internalization of HSV antigens. Effective internalization and their further presentation to antigen presenting cells (APC) are followed by mounting of antiviral response.<sup>22,26</sup>

## Conclusion

Inhibition of virus-host cell entry is an effective antiviral control strategy, which is based on the virus cell membrane adsorption, which results in inhibiting the virus activity and the ability to bind to human cells. Based on how the virus infects the host cell through interactions between viral glycoproteins and cell membrane molecules, it is possible to develop agents to counteract this process. Our results proved that the type of ligand present on the surface of NPs plays a key role in tuning the interaction between functional NPs with the viral spike proteins. Our research revealed that the use of heparin mimic ligand to disrupt the interaction between viral glycoproteins and the host cell membrane molecules is not sufficient to construct an effective virucidal preparation based on NPs. Much more effective revealed to be the use of tannic acid as NPs ligand, which ensures the affinity for viral spike proteins, exhibit very strong virucidal effect, and is non-toxic for host cells. Our work indicates that NPs functionalized with tannic acid (TA-AgNPs) have a very strong virucidal effect, much stronger than sulfonate NPs (MUS-AgNPs). Although MUS-AgNPs have a high affinity for the virus surface, they do not have a sufficient virucidal effect, and can only be called virusostatic. The results obtained in vitro were not reflected by tests performed in vivo, indicating that virusostatic effect may not be sufficient to show any antiviral activity in vivo. These effects may be due to the specific character of interaction between tannic acid and HSV glycoproteins, or other factors influencing activity of sulfonate NPs such as stability in tissue environment, corona effects and others. Our research indicates stronger virucidal effect of TA-AgNPs, related to the destruction of the structure/integrity of the virus membrane and the unwinding of the DNA strands. These results clearly indicate the effectiveness of TA-AgNPs in combating of HSV-2 infections and maybe also the other viral infections.

## Ethics

The animal study protocol was approved by the Local Committee on the Ethics of Animal Experiments in Warsaw, Poland (permit Number: WAW2/69/2021).

## Funding

This work was supported by the National Science Centre, Poland (UMO 2018/31/B/NZ6/02606).

## Disclosure

The authors report no conflicts of interest in this work.

## References

- Withley RJ, Baron S. Medical Microbiology. 4th edition. Galveston (TX): University of Texas Medical Branch at Galveston; 1996. Available from: <https://www.ncbi.nlm.nih.gov/books/NBK8157/>. Accessed February 20, 2025.
- Website who.int. Herpes simplex virus. World Health Organization. 2024. Available from: <https://www.who.int/news-room/fact-sheets/detail/herpes-simplex-virus>. Accessed December 11, 2024.
- James SH, Sheffield JS, Kimberlin DW. Mother-to-child transmission of herpes simplex virus. *J Pediatric Infect Dis Soc*. 2014;3(Suppl 1):S19–23. doi:10.1093/jpids/piu050
- Civitelli L, Marcocci ME, Celestino I. Herpes simplex virus type 1 infection in neurons leads to production and nuclear localization of APP intracellular domain (AICD): implications for Alzheimer's disease pathogenesis. *J Neurovirol*. 2015;21(5):480–490. doi:10.1007/s13365-015-0344-0
- Athanasίου E, Gargalionis AN, Anastassopoulou C, Tsakris A, Boufidou F. New insights into the molecular interplay between human herpesviruses and alzheimer's disease-a narrative review. *Brain Sci*. 2022;12(8):1010. doi:10.3390/brainsci12081010
- Laval K, Enquist LW. The potential role of herpes simplex virus type 1 and neuroinflammation in the pathogenesis of alzheimer's disease. *Front Neurol*. 2021;12. doi:10.3389/fneur.2021.658695
- Kristen H, Santana S, Sastre I, Recuero M, Bullido MJ, Aldudo J. Herpes simplex virus type 2 infection induces AD-like neurodegeneration markers in human neuroblastoma cells. *Neurobiol Aging*. 2015;36(10):2737–2747. doi:10.1016/j.neurobiolaging.2015.06.014
- Goldhardt O, Freiberger R, Dreyer T, et al. Herpes simplex virus alters Alzheimer's disease biomarkers -A hypothesis paper. *Alzheimer's Dement*. 2023;19:2117–2134. doi:10.1002/alz.12834
- Chakravarty M, Vora A. Nanotechnology-based antiviral therapeutics, drug delivery. *Transl Res*. 2021;11(3):748–787. parainfluenza virus type, Int. J. Nanomedicine 2013, 8:4303–14, doi: 10.2147/IJN.S50070. doi:10.1007/s13346-020-00818-0
- Orłowski O, Soliwoda K, Tomaszewska E, et al. Toxicity of tannic acid-modified silver nanoparticles in keratinocytes: potential for immunomodulatory applications. *Toxicology in Vitro*. 2016;35:43–54. doi:10.1016/j.tiv.2016.05.009
- Orłowski P, Kowalczyk A, Tomaszewska E. Antiviral activity of tannic acid modified silver nanoparticles: potential to activate immune response in herpes genitalis. *Viruses*. 2018;10(524). doi:10.3390/v10100524
- Orłowski P, Tomaszewska E, Ranoszek-Soliwoda K. Tannic acid-modified silver and gold nanoparticles as novel stimulators of dendritic cells activation. *Front Immunol*. 2018;9:1115. doi:10.3389/fimmu.2018.01115
- Liu L, Ge C, Zhang Y, et al. Tannic acid-modified silver nanoparticles for enhancing anti-biofilm activities and modulating biofilm formation. *Biomater Sci*. 2020;4852–4860. doi:10.1039/D0BM00648C
- Galdiero S, Falanga A, Vitiello M, Cantisani M, Marra V, Galdiero M. Silver nanoparticles as potential antiviral agents. *Molecules*. 2011;16(10):8894–8918. doi:10.3390/molecules16108894
- Rai M, Kon K, Ingle A, Duran N, Galdiero S, Galdiero M. Broad-spectrum bioactivities of silver nanoparticles: the emerging trends and future prospects. *Appl Microbiol Biotechnol*. 2014;98(5):1951–1961. doi:10.1007/s00253-013-5473-x
- Gaikwad S, Ingle A, Gade A, et al. Antiviral activity of mycosynthesized silver nanoparticles against herpes simplex virus and human. *Int J Nanomedicine*. 2013;8:4303–4314. doi:10.2147/IJN.S50070
- Al-Karmalawy AA, El-Gamil DS, El-Shesheny R, et al. Design and statistical optimisation of emulsomal nanoparticles for improved anti-SARS-CoV-2 activity of N-(5-nitrothiazol-2-yl)-carboxamido candidates: in vitro and in silico studies. *Journal of Enzyme Inhibition and Medicinal Chemistry*. 2023;38(1). doi:10.1080/14756366.2023.2202357
- Zakaria MY, Zaki I, Alhomrani M, Alamri AS, Abdulaziz O, Abourehab MAS. Boosting the anti MERS-CoV activity and oral bioavailability of resveratrol via PEG-stabilized emulsomal nano-carrier: factorial design, in-vitro and in-vivo assessments. *Drug Deliv*. 2022;29(1):3155–3167. doi:10.1080/10717544.2022.2126028
- Zakaria MY, El-Halim SM SMA, Beshay BY, Zaki I, Abourehab MAS. 'Poly phenolic phytoceutical loaded nano-bilosomes for enhanced caco-2 cell permeability and SARS-CoV 2 antiviral activity': in-vitro and insilico studies. *Drug Deliv*. 2023;30(1):2162157. doi:10.1080/10717544.2022.2162157
- Tomaszewska E, Ranoszek-Soliwoda K, Bednarczyk K. Anti-HSV activity of metallic nanoparticles functionalized with sulfonates vs. polyphenols. *Int J Mol Sci*. 2022;23(21):13104. doi:10.3390/ijms232113104
- Papp I, Sieben C, Ludwig K, et al. Inhibition of influenza virus infection by multivalent sialic-acid-functionalized gold nanoparticles. *Small*. 2010;6(24):2900–2906. doi:10.1002/smll.201001349
- Orłowski P, Tomaszewska E, Gniadek M, et al. Tannic acid modified silver nanoparticles show antiviral activity in herpes simplex virus type 2 infection. *PLoS One*. 2014;9(8):e104113. doi:10.1371/journal.pone.0104113
- Cagno V, Andreozzi P, D'Alicarnasso M, et al. Broad-spectrum non-toxic antiviral nanoparticles with a virucidal inhibition mechanism. *Nat Mater*. 2018;17(2):195–203. doi:10.1038/nmat5053



24. Deng P, Athary Abdulhaleem MF, Masoud RE, Alamoudi WM, Zakaria MY. Employment of PEGylated ultra-deformable transferosomes for transdermal delivery of tapentadol with boosted bioavailability and analgesic activity in post-surgical pain. *Int J Pharm.* 2022;628:122274. doi:10.1016/j.ijpharm.2022.122274
25. Domeradзка-Gajda K, Nocun M, Roszak J. A study on the in vitro percutaneous absorption of silver nanoparticles in combination with aluminum chloride, methyl paraben or di-n-butyl phthalate. *Toxicology Letters.* 2017;272:38–48. doi:10.1016/j.toxlet.2017.03.006
26. Krzyzowska M, Janicka M, Chodkowski M. Epigallocatechin gallate-modified silver nanoparticles show antiviral activity against herpes simplex type 1 and 2. *Viruses.* 2023;15. doi:10.3390/v15102024
27. Liu T, Zhang L, Joo D, et al. NF- $\kappa$ B signaling in inflammation. *Sig Transduct Target Ther.* 2017;2:17023. doi:10.1038/sigtrans.2017.23S
28. Krzyzowska M, Kowalczyk A, Skulska K, Thörn K, Eriksson K. Fas/FasL contributes to HSV-1 brain infection and neuroinflammation. *Front Immunol.* 2021;12:714821. doi:10.3389/fimmu.2021.714821
29. Bieñ K, Sokołowska J, Baska P, Nowak Z, Stankiewicz W, Krzyzowska M. Fas/FasL pathway participates in regulation of antiviral and inflammatory response during mousepox infection of lungs. *Mediators Inflamm.* 2015;2015:281613. doi:10.1155/2015/281613
30. Abdellatif AA, Rasheed Z, Alhowail AH. Silver citrate nanoparticles inhibit PMA-induced TNF $\alpha$  expression via deactivation of NF- $\kappa$ B activity in human cancer cell-lines, MCF-7. *Int J Nanomedicine.* 2020;15:8479–8493. doi:10.2147/IJN.S274098
31. Vendidandala NR, Yin TP, Nelli G, Pasupuleti VR, Nyamathulla S, Mokhtar SI. Gallic acid silver nanoparticle impregnated cotton gauze patches enhance wound healing in diabetic rats by suppressing oxidative stress and inflammation via modulating the Nrf2/HO-1 and TLR4/NF- $\kappa$ B pathways. *Life Sci.* 2021;286:120019. doi:10.1016/j.lfs.2021.120019
32. Schiffer JT, Corey L. *Mandell, Douglas, and Bennett's Principles and Practice of Infectious Diseases (Eighth Edition).* 2015.
33. Ghaffari H, Tavakoli A, Moradi A, et al. Inhibition of H1N1 influenza virus infection by zinc oxide nanoparticles: another emerging application of nanomedicine. *J Biomed Sci.* 2019;26(1):70. doi:10.1186/s12929-019-0563-4
34. Trybala E, Liljeqvist J-Å, Svennerholm B, Bergström T. Herpes simplex virus types 1 and 2 differ in their interaction with heparan sulfate. *J Virol.* 2000;74(19):9106–9114. doi:10.1128/jvi.74.19.9106-9114.2000
35. Rusnati M, Vicenzi E, Donalizio M, Oreste P, Landolfo S, Lembo D. Sulfated K5 Escherichia coli polysaccharide derivatives: a novel class of candidate antiviral microbicides. *Pharmacol Ther.* 2009;123(3):310–322. doi:10.1016/j.pharmthera.2009.05.001
36. Mycroft-West CJ, Su D, Pagani I, et al. Heparin inhibits cellular invasion by SARS-CoV-2: structural dependence of the interaction of the spike S1 receptor-binding domain with heparin. *Thromb Haemost.* 2020;120(12):1700–1715. doi:10.1055/s-0040-1721319
37. Schandock F, Riber CF, Röcker A, et al. Macromolecular antiviral agents against zika, Ebola, SARS, and other pathogenic viruses. *Adv Healthc Mater.* 2017;6(23):1700748. doi:10.1002/adhm.201700748
38. Gerber SI, Belval BJ, Herold BC. Differences in the role of glycoprotein C of HSV-1 and HSV-2 in viral binding may contribute to serotype differences in cell tropism. *Virology.* 1995;214(1):29–39. doi:10.1006/viro.1995.9957
39. Herold BC, WuDunn D, Soltys N, Spear PG. Glycoprotein C of herpes simplex virus type 1 plays a principal role in the adsorption of virus to cells and in infectivity. *J Virol.* 1991;65(3):1090–1098. doi:10.1128/JVI.65.3.1090-1098.1991
40. Tal-Singer R, Peng C, Ponce De Leon M, et al. Interaction of herpes simplex virus glycoprotein gC with mammalian cell surface molecules. *J Virol.* 1995;69(7):4471–4483. doi:10.1128/JVI.69.7.4471-4483.1995
41. Neli V-I, Galabov AS, Mileva M. Tannins as antiviral agents. In: *Tannins - Structural Properties, Biological Properties and Current Knowledge.* IntechOpen; 2020. doi:10.5772/intechopen.86490
42. Isenburg JC, Simionescu DT, Vyavahare NR. Tannic acid treatment enhances biostability and reduces calcification of glutaraldehyde fixed aortic wall. *Biomaterials.* 2005;26(11):1237–1245. doi:10.1016/j.biomaterials.2004.04.034
43. Lin LT, Chen TY, Lin SC, et al. Broad-spectrum antiviral activity of chebulagic acid and punicalagin against viruses that use glycosaminoglycans for entry. *BMC Microbiol.* 2013;13:187. doi:10.1186/1471-2180-13-187
44. Chaudhuri A, Battaglia G, Golestanian R. The effect of interactions on the cellular uptake of nanoparticles. *Phys Biol.* 2011;8(4):046002. doi:10.1088/1478-3975/8/4/046002
45. Lipowsky R, Döbereiner HG. Vesicles in contact with nanoparticles and colloids. *Europhys Lett.* 1998;43:219225. doi:10.1209/epl/i1998-00343-4
46. Xie YW, Xu HX, Dong H, Fiscus RR, But PP. Role of nitric oxide in the vasorelaxant and hypotensive effects of extracts and purified tannins from *Geum japonicum*. *J Ethnopharmacol.* 2007;109(1):128–133. doi:10.1016/j.jep.2006.07.015
47. Fukuchi K, Sakagami H, Okuda T, et al. Inhibition of herpes simplex virus infection by tannins and related compounds. *Antiviral Res.* 1989;11:285. doi:10.1016/0166-3542(89)90038-7
48. Reshamwala D, Shroff S, Sheik Amamuddy O. Polyphenols epigallocatechin gallate and resveratrol, and polyphenol-functionalized nanoparticles prevent enterovirus infection through clustering and stabilization of the viruses. *Pharmaceutic.* 2021;13(8):1182. doi:10.3390/pharmaceutics13081182
49. Lin LT, Chen TY, Chung CY, et al. Hydrolyzable tannins (chebulagic acid and punicalagin) target viral glycoprotein-glycosaminoglycan interactions to inhibit herpes simplex virus 1 entry and cell-to-cell spread. *J Virol.* 2011;85(9):4386–4398. doi:10.1128/JVI.01492-10